10-1-2005

Damage-Induced Modeling of Asphalt Mixtures through Computational Micromechanics and Cohesive Zone Fracture

Yong-Rak Kim
University of Nebraska - Lincoln, yong-rak.kim@unl.edu

D. H. Allen
University of Nebraska-Lincoln, dallen3@unl.edu

D. N. Little
Texas A&M University, College Station, TX

Published in *Journal of Materials in Civil Engineering* 17:5 (October 1, 2005), pp. 477–484;
doi 10.1061/(ASCE)0899-1561(2005)17:5(477)

Submitted September 3, 2003; accepted June 7, 2004.

Damage-Induced Modeling of Asphalt Mixtures through Computational Micromechanics and Cohesive Zone Fracture

Yong-Rak Kim, A.M.ASCE,[1] D. H. Allen,[2] and D. N. Little, F.ASCE [3]

[1] Assistant Professor, Department of Civil Engineering, University of Nebraska–Lincoln, Lincoln, NE 68588-0642

[2] Professor, Department of Engineering Mechanics, University of Nebraska–Lincoln, Lincoln, NE 68588-0642

[3] Professor, Department of Civil Engineering, Texas A&M University, College Station, TX 77843-3135

Abstract

This paper presents a computational micromechanics modeling approach to predict damage-induced mechanical response of asphalt mixtures. Heterogeneous geometric characteristics and inelastic mechanical behavior were taken into account by introducing finite element modeling techniques and a viscoelastic material model. The modeling also includes interface fracture to represent crack growth and damage evolution. The interface fracture is modeled by using a micromechanical nonlinear viscoelastic cohesive-zone constitutive relation. Fundamental material properties and fracture characteristics were measured from simple laboratory tests and then incorporated into the model to predict rate-dependent viscoelastic damage behavior of the asphalt mixture. Simulation results demonstrate that each model parameter significantly influences the mechanical behavior of the overall asphalt mixture. Within a theoretical framework of micromechanics, this study is expected to be suitable for evaluating damage-induced performance of asphalt mixtures by measuring only material properties and fracture properties of each mix component and not by recursively performing expensive laboratory tests that are typically required for continuum damage mechanics modeling.

Keywords: damage, models, asphalt mixes, viscoelasticity, micromechanics, finite element method, fractures

Introduction

As shown in Figure 1, asphalt mixtures are a multiphased particle- reinforced composite consisting of irregularly shaped and randomly oriented aggregate particles embedded in an inelastic matrix that is known to degrade with time and under mechanical, thermal, and environmental loads. The asphalt mixtures generally exhibit extremely complicated mechanical behavior and numerous damage modes. Precise identification of the damage-induced behavior of the asphalt mixtures is a challenge; however, it should be understood in an appropriate way to meet design allowables. Damage-induced constitutive modeling of asphalt mixtures is a complex subject. The difficulties in developing appropriate models are caused by complex heterogeneity and inelastic behavior of the asphalt mixtures. Because of the uncountable number of combinations in mixture design and loading conditions, it is obviously inappropriate to analyze and characterize damage-induced behavior of asphalt mixtures only by performing expensive laboratory experiments recursively. Well-defined analytical or computational models are therefore necessary.

Continuum-damage mechanics is one of theories that has been used to model damage-induced behavior of asphalt mixtures. Park et al. (1996) and Lee et al. (2000) developed continuum-damage mechanics-based models for asphalt concrete mixtures that are based on Schapery's (1984) extended elastic-viscoelastic correspondence principle. They hypothesized that phenomenologically determined internal state variables, which are determined from testing results, can be used to represent the overall locally averaged amount of damage in the sample. The continuum-damage models successfully predict structural degradation attributable to damage, but the models have limitations. Since the modeling parameters are determined from testing an asphalt mixture and the testing is based on an assumption that the sample is a statistically homogeneous continuum, each sample fabricated from different mixes of constituents requires its own constitutive tests and performance tests. The continuum-damage mechanics modeling is fairly mixture-specific and requires a new set of experiments to obtain the model parameters for each new mix.

However, micromechanics-based models, which are employed for this study, do not require a new set of experiments for a new mix, since the modeling approach is based on individual material properties and fracture properties of each mix component. Furthermore, the micromechanics approach has a unique characteristic that is based on the concept of representative volume element (RVE). Mechanical analyses of a large-scale heterogeneous asphalt mixture can be reasonably converted to mechanical analyses of a small-scale heterogeneous body (typically referred to as the RVE), since the selected scale is sufficient to reflect the overall behavior of the large-scale body. Micromechanics-based modeling has typically been implemented with the help of well-established computational techniques to solve composite media that exhibit extremely

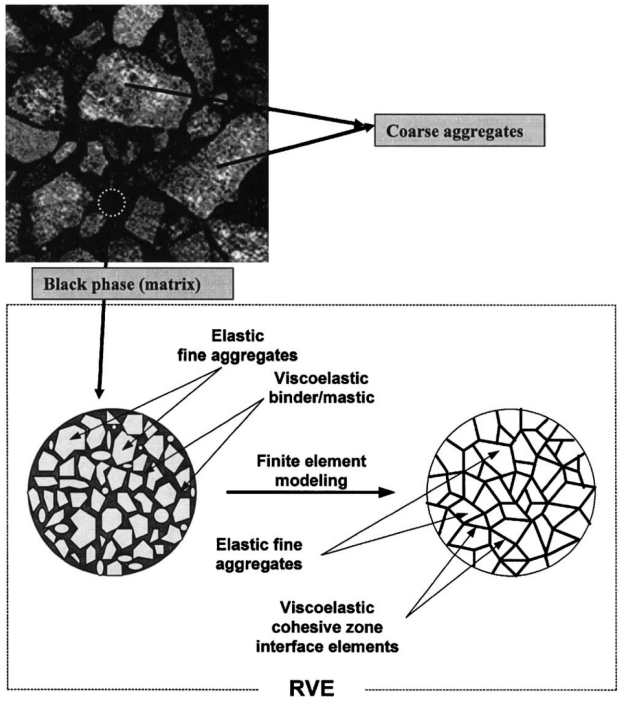

Figure 1. Typical dense-graded asphalt concrete mixture and its representation for finite element model, including cohesive-zone interface elements to reflect damage evolution.

complex phase geometry and such inelastic mechanical behavior as viscoelasticity. Guddati et al. (2002) proposed a lattice-based micromechanical model to characterize the cracking performance of asphalt concrete. By employing a random truss lattice mesh, they simulated damage evolution and crack propagation in elastic asphalt concrete samples under an indirect tensile test. The macrocracking patterns from the lattice-mesh computational simulation were in good agreement with the pattern observed from the tested sample. Sadd et al. (2003) simulated the damage behavior of asphalt concrete samples under indirect tension loading with the ABAQUS finite element program by incorporating a damage-mechanics–based softening model to predict the stiffness reduction attributable to damage evolution. However, the model does not include material viscoelasticity and rate-dependent damage growth, which are typical phenomena in asphalt mixtures. Another computational micromechanics-based modeling effort was recently conducted by Soares et al. (2003). This approach used the finite element method in an attempt to represent inhomogeneous characteristics of aggregate particles in asphalt mixtures. Asphalt binder and coarse aggregates were considered elastic, and damage evolution was modeled by introducing interface elements to represent crack growth. The authors employed a rate-independent cohesive-zone fracture model that was developed by Tvergaard (1990) to simulate crack growth at the interface elements. This approach may therefore not be sufficient for asphalt mixtures that exhibit inelastic behavior and rate-dependent damage evolution characteristics. Several studies (Costanzo and Walton 1997; Lagoudas et al. 1998) have recognized the importance of including rate dependence in the cohesive-zone fracture law, especially for such inelastic materials as asphalt mixtures. Material viscoelasticity has been reflected in the recent studies by Papagiannakis et al. (2002) and Birgisson et al. (2002). These studies successfully predict the time-dependent viscoelastic creep behavior of asphalt mixtures. However, they may not accurately model rate-dependent stiffness reduction caused by significant damage, since they do not account for path- and rate-dependent energy dissipation as microcracks initiate and propagate.

The typical asphalt concrete mixture shown in Figure 1 exhibits two distinct phases: white signifies coarse aggregate particles and black (matrix phase) signifies a combination of asphalt binder, air voids, fine aggregates, and filler. The quality of the matrix mostly influences damage and fracture of the overall asphalt mixtures, since the damage initiates with such microdamage as microcracking in the matrix. Therefore, mixture performance can be improved if the damage-affected behavior of the matrix can be well- predicted and if it is engineered to resist damage and fracture. The matrix material can be modeled as a type of particulate composite consisting mainly of viscoelastic asphalt binder (or mastic, which is a combination of binder and filler) and elastic fine aggregates.

The objective of this study is to model damage evolution in the matrix phase of asphalt mixtures. By introducing an elastic particle phase signifying fine aggregates and viscoelastic interfaces surrounding the particles signifying asphalt binder or mastic, inelastic damage growth is predicted. The finite element method—one of several computational approaches—was used in this study. The inelastic damage evolution is characterized by employing a micromechanical nonlinear viscoelastic cohesive-zone model (Yoon and Allen 1999) and fracture-test-based probabilistic damage evolution law (Allen and Searcy 2001). Material properties and fracture characteristics, which are measured from laboratory tests, were incorporated into the finite element model. This research approach is expected to be suitable for evaluating rate-dependent damage-induced performance of asphalt mixtures by using only fundamental material properties and fracture properties rather than by performing expensive laboratory tests.

Cohesive-Zone Model and Damage Evolution Law

The cohesive zones are modeled by employing interface elements, as shown in Figure 1, to model the growth of the new boundary surface both internal and external to the body through incorporating the damage evolution law. In 1999, Yoon and Allen proposed a damage-dependent constitutive model for a rate- dependent cohesive zone in a thermoviscoelastic solid. By using the Helmholtz free energy for a nonlinear viscoelastic material, the cohesive-zone constitutive equation can be constructed, with the resulting constitutive model containing an internal state variable representing damage evolution within the cohesive zone. As a subsequent effort, Seidel (2002) proposed a simpler form to reduce considerable numerical implementation from the original cohesive-zone model of Yoon and Allen (1999). The cohesive- zone model for two-dimensional problems can be expressed by

$$T_i(t) = [1 - \alpha(t)]\left[\sigma_i^f + \frac{1}{\delta_i}\int_0^t E^c(t-\xi)\frac{\partial u_i(\xi)}{\partial \xi}d\xi\right] \quad (i = n \text{ or } t) \tag{1}$$

where $T_i(t)$ = cohesive-zone area-averaged traction; $u_i(t)$ = cohesive-zone displacement; δ_i = cohesive-zone material length parameter; $\alpha(t)$ = internal state variable representing damage evolution; σ_i^f = requisite stress level to initiate cohesive zone; $E^c(t)$ = linear viscoelastic relaxation modulus of the cohesive zone; n = normal direction; and t = tangential direction.

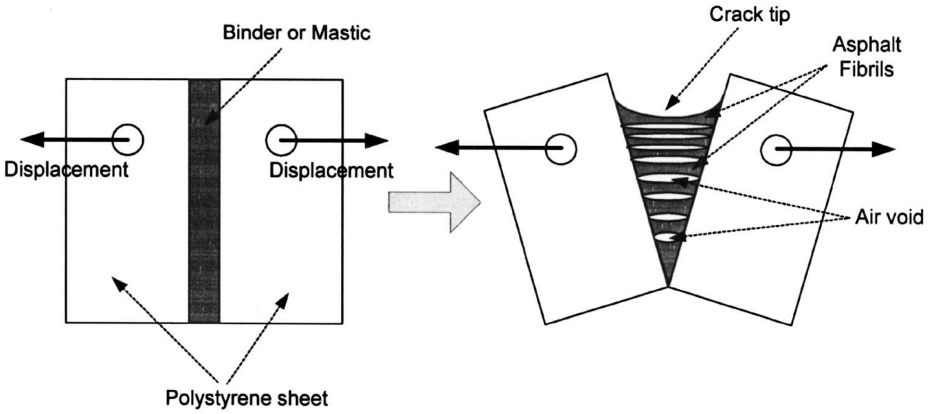

Figure 2. Schematic diagram of tensile fracture test.

The linear viscoelastic relaxation modulus of the cohesive zone $E^c(t)$ is determined by laboratory relaxation test, the results of which can be represented by a Prony series as

$$E^c(t) = E_\infty + \sum_{j=1}^{p} E_j \exp\left(-\frac{E_j}{\eta_j}t\right) \tag{2}$$

where E_∞ and E_j = spring constants; η_j = dashpot constants; and p = number of dashpots. The ratio of dashpot constants to spring constant is generally refereed to as relaxation time.

Damage evolution is characterized by the internal state variable $\alpha(t)$. The damage evolution law can typically be determined by performing fracture tests to represent the locally averaged cross-sectional area of damaged material in a cohesive zone. A testing protocol using tensile fracture tests of asphalt binders and mastics was developed by Williams (2001). A schematic diagram of the test is shown in Figure 2. As the tensile displacement increases, the binder/mastic forms cracks and a cohesive zone ahead of the crack tip. Crack-tip propagation and cohesive-zone evolution are represented by the formation of fibrils. As the cohesive zone evolves, the fibrils grow in length but reduce in cross- sectional area. The variation of the fibril geometry can be employed as an internal state variable $\alpha(t)$

$$\alpha(t) = \frac{A - \Sigma_{k=1}^{N} A_k(t)}{A} \tag{3}$$

where A = total cross-sectional area; A_k = cross-sectional area of kth fibril; and N = number of fibrils.

By assuming the geometry of each fibril to be a right circular cylinder, we can express the cross-sectional area and radius of the kth fibril including Poisson's effect as a function of time (Allen and Searcy 2001)

$$A_k(t) = \pi(r_k^o)^2[1 - \nu\lambda(t)]^2 \tag{4}$$

$$r_k(t) = r_k^o[1 - \nu\lambda(t)] \tag{5}$$

where r_k^0 = initial radius of kth fibril; v = Poisson's ratio (assumed to be independent of time); and λ = strainlike term, which is a normalized quantity coupling normal and tangential behavior.

It is further assumed that the distribution of fibril radii in the whole cohesive zone is governed by a normal distribution (Allen and Searcy 2001), $f(r(t), \zeta)$, such that

$$f(r(t),\zeta) = \frac{1}{\zeta\sqrt{2\pi}} \exp\left[\frac{-\{r - r(t)\}^2}{2\zeta^2}\right] \tag{6}$$

where $r(t)$ = average value of fibril radii at time t; and ζ = standard deviation of fibril radii (assumed to be independent of time).

Figure 3 illustrates a graphical depiction of Equation (6). As damage evolves, the average fibril radius and distribution curve will correspondingly move to the left, since all fibrils will become thinner because of damage. The distribution curve eventually passes a boundary that is marked as a critical fibril radius, r_{cr}. The area under the curve and left of the critical fibril radius represents the measure of fibril breakage or damage. It leads to the following expression for the internal state variable $\alpha(t)$ instead of Equation (3):

$$\alpha(t) = 1 - \int_{r_{cr}}^{\infty} f(r(t),\zeta)dr \tag{7}$$

Substituting Equations (5) and (6) into Equation (7) yields

$$\alpha(t) = 1 - \frac{1}{\zeta\sqrt{2\pi}} \int_{r_{cr}}^{\infty} \exp\left[\frac{-\{r - r^o[1 - \nu\lambda(t)]\}^2}{2\zeta^2}\right]dr \tag{8}$$

where r^0 =average value of initial fibril radii.

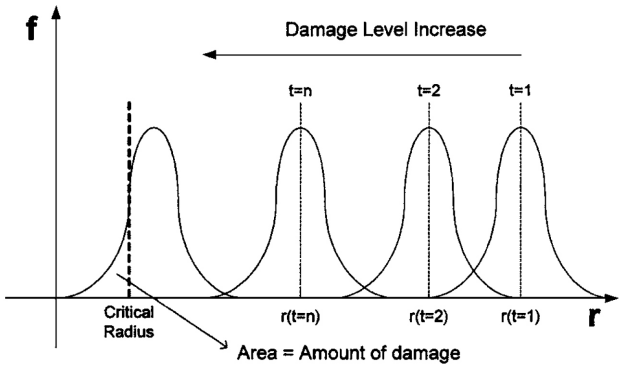

Figure 3. Graphical depiction of probabilistic distribution (normal distribution) representing fibril radii reduction and cohesive-zone evolution.

Numerical Implementation and Finite Element Formulation

In Equation (1), the viscoelastic constitution of the cohesive-zone model is expressed as a time-and history-dependent integral. In an attempt to formulate the viscoelastic constitution into a computational finite element model, it must be incrementalized so that the history dependence is retained at each time step. Suppose that the traction at time t is known and that the traction at $t + \Delta t$ is evaluated. The resulting recursive cohesive-zone traction difference ΔT_i between time t and $t + \Delta t$ can be expressed as

$$\Delta T_i = k_{ij}\Delta u_j + \Delta T_i^R \tag{9}$$

where

$$k_{ij} = \frac{[1-\alpha(t+\Delta t)]}{\delta_i}[E(\Delta t)] \tag{10}$$

$$\Delta T_i^R = \frac{[1-\alpha(t)]}{\delta_i}\left[-\sum_{j=1}^{p}\left\{1-\exp\left(-\frac{E_j}{\eta_j}\Delta t\right)\right\}\sigma_j(t)\right] - \frac{\Delta\alpha}{\delta_i}\left[E_\infty u_i(t) + \sum_{j=1}^{p}\sigma_j(t) - \sum_{j=1}^{p}\left\{1-\exp\left(-\frac{E_j}{\eta_j}\Delta t\right)\right\}\sigma_j(t)\right] + [-\Delta\alpha]\sigma_i^f \tag{11}$$

$$E(\Delta t) = E_\infty + \frac{1}{\Delta t}\sum_{j=1}^{p}\eta_j\left[1-\exp\left(-\frac{E_j}{\eta_j}\Delta t\right)\right] \tag{12}$$

$$\sigma_j(t) = \exp\left(-\frac{E_j}{\eta_j}\Delta t\right)[\sigma_j(t-\Delta t)] + \frac{\Delta\lambda}{\Delta t}\eta_j\left[1-\exp\left(-\frac{E_j}{\eta_j}\Delta t\right)\right] \tag{13}$$

If the cohesive zone is specified as a linear elastic material, the residual traction ΔT_i^R is excluded and the stiffness coefficient k_{ij} is not associated with viscoelastic time dependence. A more detailed description of the numerical implementation can be found elsewhere (Zocher et al. 1997; Seidel 2002).

In this study, the fine aggregate particles are assumed to follow linear elastic behavior. Time-incrementalized numerical form of the fine aggregate particles is therefore expressed as

$$\Delta\sigma_{ij} = C_{ijkl}\Delta\varepsilon_{kl} \tag{14}$$

where $\Delta\sigma_{ij}$ = stress increment during the time step; C_{ijkl} = time-independent elastic modulus tensor; and $\Delta\varepsilon_{kl}$ = strain increment during the time step.

The finite element model was similarly derived on the basis of a time-incrementalized numerical scheme to represent viscoelastic material characteristics. The stress, strain, and displacement at time t are assumed to be known; and the state variables at time $t + \Delta t$ are evaluated. After the strain-displacement operator, $\{\Delta\varepsilon\} = [B]\{\Delta u\}$, and the displacement shape function, $\{\Delta u\} = [N]\{\Delta U\}$ are applied, the resulting finite element formulation is finally presented in matrix form as

$$[K^e]\{\Delta U^e\} = \{f_1^e\} + \{f_2^e\} + \{f_3^e\} + \{f_4^e\} \tag{15}$$

where

$$[K^e] = \int_V [B]^T[C][B]dV + \int_{\partial V_c}[N]^T[k][N]dS \tag{16}$$

$$\{f_1^e\} = \int_{\partial V_e}[N]^T[T(t+\Delta t)]dS \tag{17}$$

$$\{f_2^e\} = -\int_V [B]^T[\sigma(t)]dV \tag{18}$$

$$\{f_3^e\} = -\int_{\partial V_c}[N]^T[T(t)]dS \tag{19}$$

and

$$\{f_4^e\} = -\int_{\partial V_c}[N]^T[\Delta T^R]dS \tag{20}$$

$[K^e]$ = element stiffness matrix, including the effects from neighboring cohesive zones; and $\{f_1^e\}$, $\{f_2^e\}$, $\{f_3^e\}$, and $\{f_4^e\}$ are contributions to the element force vector caused by surface tractions, stresses at the previous time step, cohesive-zone tractions at the previous time step, and change of cohesive-zone tractions during the time step, respectively. The second term in the element stiffness matrix and force-vector terms $\{f_3^e\}$ and $\{f_4^e\}$ are excluded if the cohesive-zone interface elements are not specified in the body. It can be noted that $\{f_4^e\}$ is a term attributable to viscoelastic characteristics from viscoelastic cohesive-zone interface elements. Part of the body can be elastic, but is still implemented in a time-incremental form.

An in-house finite element program called SAD-YKIM, which is a modified version of SADISTIC (structural analysis of damage induced stresses in thermo-inelastic composites; Allen et al. 1994) has been developed to solve structural problems that include the effects of viscoelastic cohesive-zone damage growth. To simplify calculations in the finite element code, only two- dimensional, plane stress, and plane strain formulations are implemented in the code.

Materials, Laboratory Tests, and Results

A strategic highway research program (SHRP)-classified asphalt binder AAM-1 was mixed with 25% volume fraction of limestone filler to form asphalt mastic. The limestone filler was selected because it is a popular filler. Two main categories of tests were performed, including constitutive tests to determine the linear viscoelastic material properties of the mastic (AAM-1 mixed with limestone filler) and fracture tests to determine fracture parameters. The linear viscoelastic material properties and fracture parameters resulting from laboratory tests were then incorporated into the finite element model.

The dynamic shear rheometer (DSR) was used to characterize linear viscoelastic properties of the asphalt mastic. A disc-shaped DSR specimen 2-mm high with an 8-mm diameter was placed between two plates of the DSR, and a constant shear stress that is small enough not causing any nonlinear damage was then applied to determine linear viscoelastic creep behavior. Long-term creep behavior of a specimen was determined by applying the time- temperature superposition concept with individual isothermal creep data at three temperatures: 10, 31, and 40°C. The individual creep test at each temperature was performed to measure data starting from 0.01 to 1,000 s. Figure 4 illustrates reduced master plots at 25°C after superposition of individual creep data at different temperatures. A

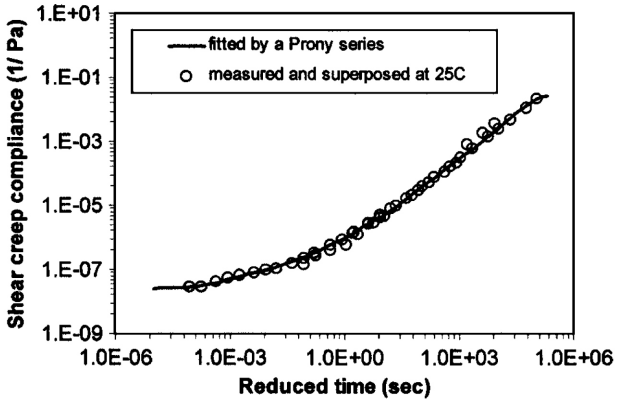

Figure 4. Reduced master curve at 25° C after superposition and Prony series fit.

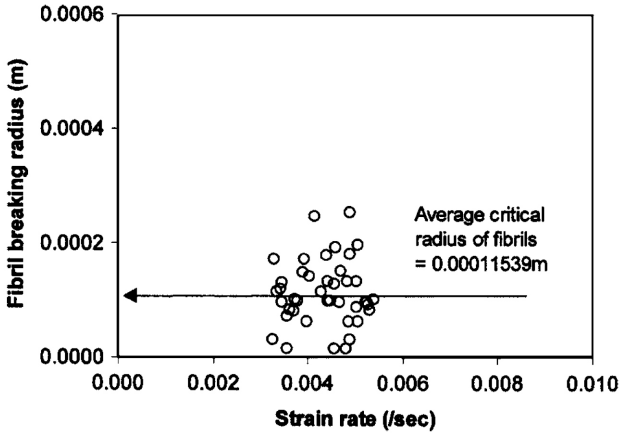

Figure 5. Tensile fracture testing results.

master shear creep curve at 25°C was then fitted by a Prony series mathematical representation. Prony series constants determined from the shear creep curve were then converted into Prony series constants in terms of the relaxation modulus, since the finite element formulation is presented in terms of the modulus. Table 1 presents Prony series parameters in terms of relaxation behavior that is converted from the creep behavior based on linear viscoelastic theory.

As previously mentioned, damage evolution is characterized by the internal state variable, and the damage evolution law can be reasonably determined by performing fracture tests. In this study, a testing protocol using tensile fracture tests developed by Williams (2001) was used to monitor damage evolution and to define the cohesive-zone damage evolution law of the asphalt mastic. Continuous fibril development and cohesive-zone growth because of damage were captured by using an optical microscope and analyzed by producing video images. The length, size, and width of the fibrils were tracked by pixel counts in the image analysis. By measuring opening displacements and fibril- geometry variation of the cohesive-zone probabilistic damage evolution law, Equation (8) can be defined. Figure 5 presents tensile fracture testing results. As demonstrated in the figure, it can be inferred that the fibril-breaking radius is not rate-dependent, since a clear trend between the critical fibril radius and the strain rate was not observed. The average critical fibril radius and the standard deviation of fibril radii are determined as 0.0001154 m and 0.0000567 m, respectively. Significant variations in critical fibril radii were observed in this particular study. Since the average value of the critical fibril radii has been employed as a fracture criterion governing cohesive failure at the interfaces between fine aggregate particles and asphalt binder (or mastic), appropriate determination of the average value of critical fibril radii is necessary to predict the overall damage-associated mechanical behavior of asphalt mixtures. Further testing is recommended to reduce variation of the testing results.

Table 1. Viscoelastic Material Properties and Fracture Parameters

(a) Viscoelastic material properties	
ν	0.40
E_∞	0.122 kPa
E_1	73,173 kPa
2	25,506
3	10,847
4	2,078
5	332
6	53.4
7	8.44
8	1.33
9	0.252
η1	115 kPa s
2	418
3	1,079
4	1,529
5	2,249
6	3,513
7	5,430
8	8,664
9	20,406
(b) Fracture parameters	
δ ($\delta_n = \delta_t$)	0.0001 m, 0.00005 m
ro	0.0002 m, 0.0003 m
rcr	0.0001154 m, 0.0000577 m
ζ	0.0000567 m

For all cases, σ_n^f and σ_t^f are assumed to be zero.

Finite Element Mesh and Boundary Conditions

Figure 6 shows the finite element mesh to model particulate composites that are composed of fine elastic aggregate particles and the thin film of viscoelastic mastic (AAM-1 mixed with limestone filler) surrounding the aggregate particles. A Voronoi tessellation approach has been used to construct a randomly oriented grain structure. The details of the technique can be found in a study by Van der Burg and Van der Giessen (1994). A 506-particle mesh was developed as a trial representative volume element (TRVE) to investigate damage-induced mechanical behavior. The chosen TRVE is not the one from rigorous studies for RVE determination (Helms et al. 1999; Helms 2000) for this particular study. However, the 506-particle sample can be considered a well-defined RVE according to a study by Helms (2000). Helms performed comprehensive studies to determine the RVE that would be appropriate for a specific inelastic material by introducing statistical prediction techniques through a series of modeling simulations that considered the separate effects of geometry, mesh refinement, average particle size, and sample size effect. One major finding of the study was that a suitable RVE would be large enough to contain approximately 500 particles for both elastic and inelastic materials, given an average particle size. It can be inferred that the

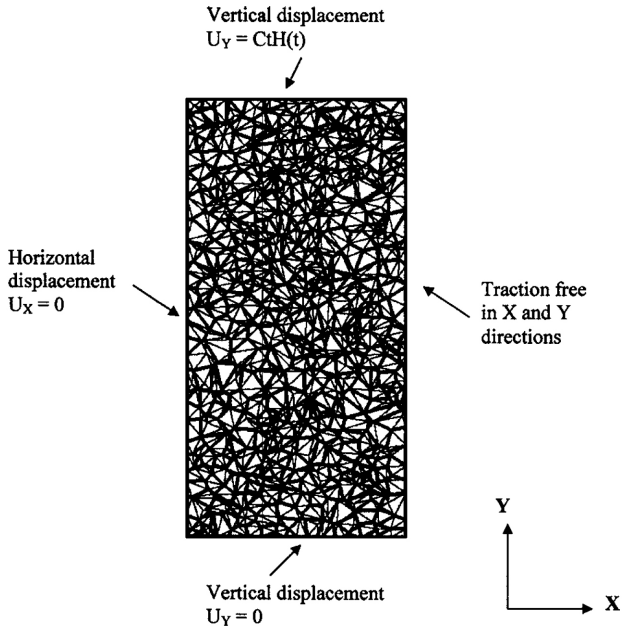

Figure 6. 506-particle finite element mesh and specified boundary conditions.

selected 506-particle volume element for this study is arbitrary but is a reasonably determined finite element mesh for representing overall damage-induced behavior of the matrix phase. The dimension of the body, 0.005 m by 0.01 m, was selected with an intention to match the particle size, which is approximately 0.3 to 0.4 mm, of the finite element mesh to the size of typical fine particles. The viscoelastic interface elements along the elastic particle boundaries are governed by the viscoelastic cohesive-zone model [Equation (1)], and damage evolution of the cohesive zones follows the probabilistic damage evolution law [Equation (8)]. Triangular elements are used because they are particularly useful in describing geometric irregularities of particles.

Boundary conditions imposed on the TRVE are also shown in Figure 6. Constant rate uniaxial displacement, $u_y = CtH(t)$, was applied on the top face monotonically to simulate damage growth attributable to the uniaxial tension. The constant C is unit displacement per second, and $H(t)$ is the Heaviside step function. Other boundary conditions associated with each face are specified in Figure 6. The traction boundary conditions are imposed along the cohesive-zone interface elements in accordance with Equation (1).

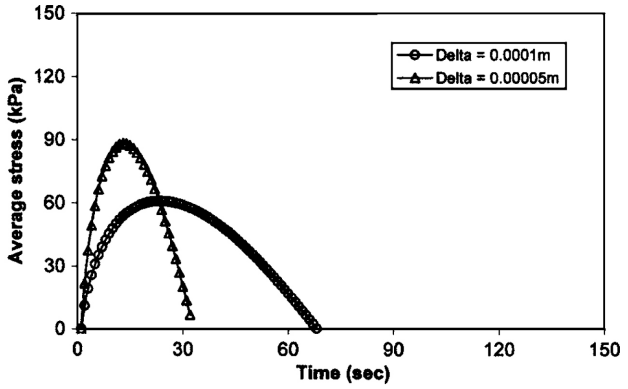

Figure 7. Effect of material length parameter on damage-induced behavior.

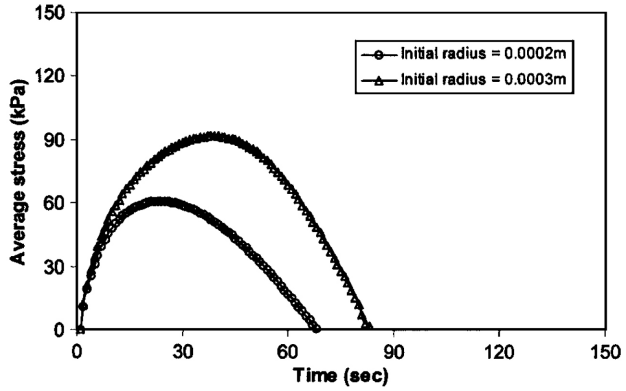

Figure 8. Effect of initial fibril radius on damage-induced behavior.

Model Simulations and Discussion

Various model simulations can be conducted by varying the model parameters. They include simulations of the material properties and fracture properties. On basis of the tensile fracture- testing results, several different values of the material length parameter (δ_n and δ_t), averaged initial fibril radius (r^0), and averaged critical fibril radius (r_{cr}) were used to investigate the sensitivities depending on damage parameters. The fine aggregate particles and asphalt mastic were assumed to follow isotropic linear elastic and isotropic linear viscoelastic behavior, respectively. An elastic modulus of 55.2 GPa of the particles was assumed, on the basis of a study by Zhou et al. (1995). Constant values of 0.40 and 0.15 were selected for the Poisson's ratios of the asphalt mastic and fine aggregate, respectively. Poisson's ratios do not vary significantly, as demonstrated in a study by Schapery (1974).

Figures 7–9 clearly demonstrate that damage-induced behavior is dependent on specified damage parameters. In Equations (1) and (8), the cohesive-zone traction induced by nodal displacements at the interface elements is influenced by the material length parameters (δ_n, δ_t) and the following damage parameters: averaged initial fibril radius (r^0), aver-

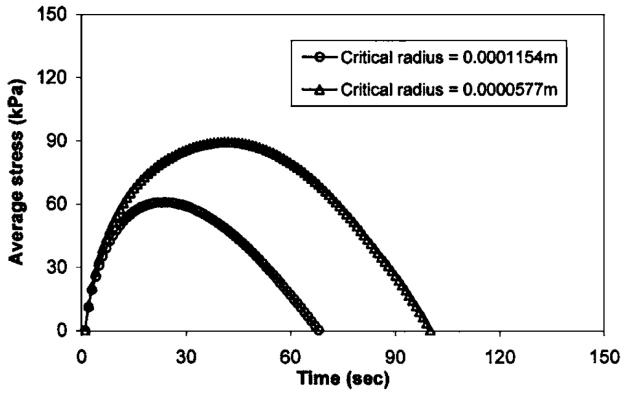

Figure 9. Effect of critical fibril radius on damage-induced behavior.

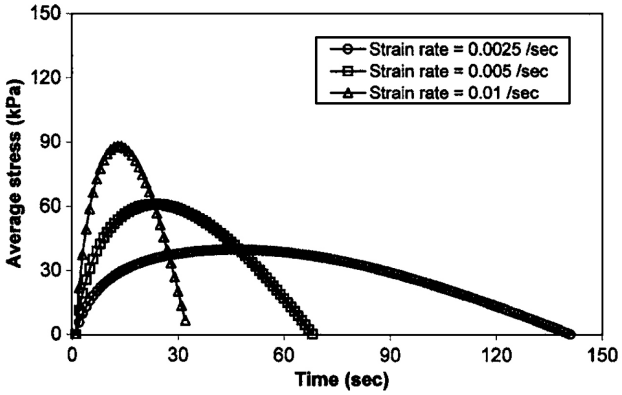

Figure 10. Effect of strain rate on damage-induced behavior.

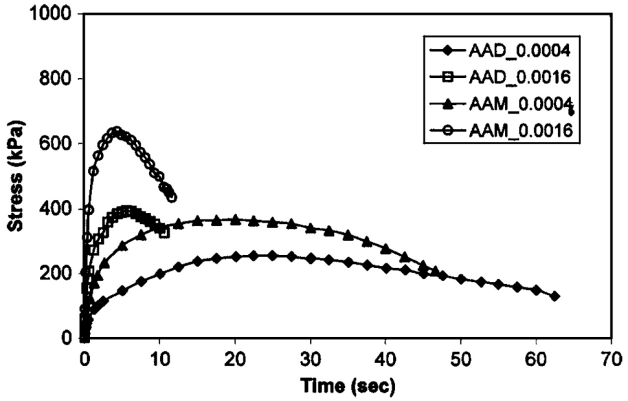

Figure 11. Constant strain-rate monotonic loading test results.

age critical fibril radius at failure (r_{cr}), and standard deviation of the fibril radii (ζ). For convenience, the same value (δ) for the length parameter was used instead of two different values (δ_n, δ_t). Figure 7 generally demonstrates that the mechanical response is stiffer and the damage growth is faster as the length-scale parameters are reduced. This finding is fairly obvious because the lower values of the length-scale parameter increase , correspondingly making the damage evolution variable $\alpha(t)$ greater. Figures 8 and 9 illustrate simulation results for different values of r^0 (averaged initial fibril radius) and r_{cr} (averaged critical fibril radius). The amount of damage evolution at a certain time becomes greater as a smaller value of the initial fibril radius is specified, since thinner fibrils approach critical fibril radius faster than thicker fibrils. Similarly, the damage evolution becomes faster as fibrils reach failure faster, which means that the value of the critical fibril radius is high. More rapid growth of damage contributes to reduction of resultant traction at the cohesive zones and a corresponding decrease in average stress of the overall composite. The geometric fibril variation of asphalt binder and mastic through the tensile fracture test appears to define damage evolution law, and the determined damage evolution characteristics subsequently predict overall matrix behavior and eventually damage-affected behavior of asphalt concrete mixtures.

In an attempt to examine rate dependency, three different strain rates—0.0025, 0.005, and 0.01/s—were applied, and simulation results are presented in Figure 10. As expected, the material response stiffens with an increasing strain rate, since the loading rate has a strong effect on the viscoelastic cohesive traction-displacement relationship. A slower loading rate produces a more compliant response because the slow loading rate gives more time for the viscous mechanisms and microstructural damage in the cohesive zone to occur. Simulation results of the damage-induced composite behavior depending on applied loading rates can be verified by Figure 11, which illustrates a series of constant strain-rate monotonic loading tests with varying strain rates for dense-graded asphalt concrete mixtures. The test results presented in Figure 11 indicate that the loading-rate-dependent nature of asphalt composites is obviously reflected in the testing results. A slower loading rate (0.0004) produces a more compliant response than a faster loading rate (0.0016). The testing results are generally compatible with the simulation predictions presented in Figure 10.

Concluding Remarks

A damage-including finite element model has been formulated herein for analyzing asphalt mixtures that are composed of elastic aggregate particles and a viscoelastic matrix. Heterogeneous geometric characteristics and inelastic mechanical behavior of the asphalt mixtures were successfully taken into account by employing a computational modeling approach and a viscoelastic material model. Crack growth attributable to damage evolution was characterized by the micromechanical nonlinear viscoelastic cohesive-zone model and fracture-test-based probabilistic damage evolution law. Locally averaged critical fibril radius as a fracture criterion on the basis of simple fracture tests looks reasonable for predicting microscale damage growth and eventually macrocracking and failure. This study is based on a micromechanics approach, so a well-defined representative volume element, fundamental material properties of each mix component, and fracture characteristics of damage-induced constituents are only required to model and predict damage-induced behavior of general asphalt mixtures. The proposed modeling approach shows great promise because of its sound theoretical and physical aspects.

Although promising results were obtained, much work remains to be done. The modeling in this study has primarily addressed the damage in the matrix phase because most damage in asphalt concrete mixtures begins in the matrix phase. However, physical and mechanical impacts of coarse aggregate particles in the mixture should be taken into account for predicting the damage behavior of asphalt concrete mixtures more accurately. The effects of aggregate gradation, particle size, angularity, texture, and particle-to-particle contacts on the mechanical response should be reflected in the overall computational model. Finite element computational simulations including the impact of coarse aggregates can be successfully obtained by using realistic finite element meshes that are based on digital images of the internal structure of asphalt concrete samples. The writers are working on such a project.

This finite element analysis has simulated only static behavior under uniaxial tension. Modeling fatigue behavior under cyclic loading conditions is recommended as a follow-up work. The current model simulates damage evolution and crack growth that is based on the nonlinear viscoelastic cohesive-zone fracture. The cohesive-zone model can be advanced by employing some other physical material properties associated with damage and crack growth. Surface energy char-

acteristics are promising candidates for model updates. Ultimately, the presented approach can be ex- panded to predict real pavement performance that is based on a micromechanical multiscale scheme (Allen 2001). The effects of microscale damage observed on the local scale analysis will be employed to estimate and predict global scale performance such as fatigue cracking and failure of asphalt concrete pavements.

Acknowledgments

The writers would like to acknowledge the Western Research Institute and the Federal Highway Administration for their financial support. Special thanks go to Dr. H. J. Lee for his monotonic uniaxial tension testing data of asphalt concrete samples.

References

Allen, D. H. (2001). "Homogenization principles and their application to continuum damage mechanics." *Compos. Sci. Technol.,* 61, 2223–2230.

Allen, D. H., Jones, R. H., and Boyd, J. G. (1994). "Micromechanical analysis of a continuous fiber metal matrix composite including the effects of matrix viscoplasticity and evolving damage." *J. Mech. Phys. Solids,* 42:3, 505–529.

Allen, D. H., and Searcy, C. R. (2001). "A micromechanically based model for predicting dynamic damage evolution in ductile polymers." *Mech. Mater.,* 33, 177–184.

Birgisson, B., Sangpetngam, B., and Roque, R. (2002). "Predicting viscoelastic response and crack growth in asphalt mixtures with the boundary element method." *Transportation Research Record. 1789,* Transportation Research Board, Washington, D.C., 129–135.

Costanzo, F., and Walton, J. R. (1997). "A study of dynamic crack growth in elastic materials using a cohesive zone model." *Int. J. Eng. Sci.,* 35, 1085–1114.

Guddati, M. N., Feng, Z., and Kim, Y. R. (2002). "Towards a micromechanics-based procedure to characterize fatigue performance of asphalt concrete." *Transportation Research Record. 1789,* Transportation Research Board, Washington, D.C., 121–128.

Helms, K. L. E. (2000). "Modeling the mechanical response and damage evolution in inelastic polycrystalline solids." PhD dissertation, Texas A&M Univ., College Station, TX.

Helms, K. L. E., Allen, D. H., and Hurtado, L. D. (1999). "A model for predicting grain boundary cracking in polycrystalline viscoplastic materials including scale effects." *Int. J. Fract.,* 95, 175–194.

Lagoudas, D. C., Ma, X., and Xu, S. (1998). "Surface damage modeling of oxidized metal matrix composite laminates under axial and transverse tension." *Int. J. Damage Mech.,* 7, 209–237.

Lee, H. J., Daniel, J. S., and Kim, Y. R. (2000). "Continuum damage mechanics-based fatigue model of asphalt concrete." *J. Mater. Civ. Eng.,* 12:2, 105–112.

Papagiannakis, A. T., Abbas, A., and Masad, E. (2002). "Micromechanical analysis of viscoelastic properties of asphalt concretes." *Transportation Research Record. 1789,* Transportation Research Board, Washington, D.C., 113–120.

Park, S. W., Kim, Y. R., and Schapery, R. A. (1996). "A viscoelastic continuum damage model and its application to uniaxial behavior of asphalt concrete." *Mech. Mater.,* 24, 241–255.

Sadd, M. H., Dai, Q., Parameswaran, V., and Shukla, A. (2003). "Simulation of asphalt materials using a finite element micromechanical model with damage mechanics." Paper Presented at 82nd Annual Meeting, Transportation Research Board, Washington, D.C.

Schapery, R. A. (1974). "Viscoelastic behavior and analysis of composite materials." *Mech. Compos. Mater.,* 2, 85–168.

Schapery, R. A. (1984). "Correspondence principles and a generalized J-integral for large deformation and fracture analysis of viscoelastic media." *Int. J. Fract.,* 25, 195–223.

Seidel, G. D. (2002). "A model for predicting the evolution of damage in the plastic bonded explosive LX17." MS thesis, Texas A&M Univ., College Station, TX.

Soares, B. J., Freitas, F., and Allen, D. H. (2003). "Crack modeling of asphaltic mixtures considering heterogeneity of the material." Paper Presented at 82nd Annual Meeting, Transportation Research Board, Washington, D.C.

Tvergaard, V. (1990). "Effect of fiber debonding in a whisker-reinforced metal." *Mater. Sci. Eng., A,* A125:2, 203–213.

Van der Burg, M. W. D., and Van der Giessen, E. (1994). "Simulation of microcrack propagation in creeping polycrystals due to diffusive grain boundary cavitation." *Appl. Mech. Rev.,* 47, 122–131.

Williams, J. J. (2001). "Two experiments for measuring specific viscoelastic cohesive zone parameters." MS thesis, Texas A&M Univ., College Station, TX.

Yoon, C., and Allen, D. H. (1999). "Damage dependent constitutive behavior and energy release rate for a cohesive zone in a thermoviscoelastic solid." *Int. J. Fract.,* 96, 55–74.

Zhou, F. P., Lydon, F. D., and Barr, B. I. G. (1995). "Effect of coarse aggregate on elastic modulus and compressive strength of high performance concrete." *Cem. Concr. Res.,* 20, 177–186.

Zocher, M. A., Allen, D. H., and Groves, S. E. (1997). "A three dimensional finite element formulation for thermoviscoelastic orthotropic media." *Int. J. Numer. Methods Eng.,* 40, 2267–2288.